Induction of Diaphragmatic Nitric Oxide Synthase after Endotoxin Administration in Rats

Role on Diaphragmatic Contractile Dysfunction

Jorge Boczkowski, Sophie Lanone, Dan Ungureanu-Longrois, Gawiyou Danialou, Thierry Fournier, and Michel Aubier
with the technical assistance of **Patricia Mechighel**
Institut National de la Santé et de la Recherche Médicale (INSERM) U408, 75870 Paris Cedex 18, France

Abstract

Nitric oxide (NO), a free radical that is negatively inotropic in the heart and skeletal muscle, is produced in large amounts during sepsis by an NO synthase inducible (iNOS) by LPS and/or cytokines. The aim of this study was to examine iNOS induction in the rat diaphragm after *Escherichia Coli* LPS inoculation (1.6 mg/kg i.p.), and its involvement in diaphragmatic contractile dysfunction. Inducible NOS protein and activity could be detected in the diaphragm as early as 6 h after LPS inoculation. 6 and 12 h after LPS, iNOS was expressed in inflammatory cells infiltrating the perivascular spaces of the diaphragm, whereas 12 and 24 h after LPS it was expressed in skeletal muscle fibers. Inducible NOS was also expressed in the left ventricular myocardium, whereas no expression was observed in the abdominal, intercostal, and peripheral skeletal muscles. Diaphragmatic force was significantly decreased 12 and 24 h after LPS. This decrease was prevented by inhibition of iNOS induction by dexamethasone or by inhibition of iNOS activity by N^G-methyl-L-arginine. We conclude that iNOS was induced in the diaphragm after *E. Coli* LPS inoculation in rats, being involved in the decreased muscular force. (*J. Clin. Invest.* 1996. 98:1550–1559.) Key words: sepsis • respiratory insufficiency • respiratory muscles • free radicals • cytokines

Introduction

Sepsis is a common cause of morbidity and mortality, particularly in the elderly, immunocompromised, and critically ill patients. Indeed, severe sepsis has been reported to be presently the most common cause of death in the noncoronary intensive care unit in the United States (1).

Respiratory failure is a major clinical manifestation of sepsis, greatly contributing to the mortality of this pathologic condition (2). Respiratory failure in this context has been traditionally related to the development of the adult respiratory distress syndrome (ARDS)[1] (2). However, recent data from experimental animals suggest that impaired contractile function of respiratory muscles, particularly the diaphragm, can also contribute to respiratory failure during sepsis (3–7). Sepsis may also play an important contributive role in diaphragmatic contractile impairment in human pathology, especially in patients in whom impaired respiratory muscle function is critical, such as patients with malnutrition (8), neuromuscular disorders (9), and chronic obstructive lung disease (10) and during weaning from mechanical ventilation (11).

Nitric oxide (NO) plays an important role in many biological functions (12). NO is derived from the oxidation of the terminal guanidino nitrogen atom of L-arginine by NO synthase (NOS), of which three isoforms have been cloned (reviewed in reference 13). Two are constitutive: the endothelial and brain isoforms (eNOS and bNOS, respectively). The third isoform is inducible (iNOS) upon stimulation by LPS and/or cytokines and leads to the production of large quantities of NO. Recent studies have shown that overproduction of NO by iNOS plays a crucial role in the pathophysiology of sepsis. Indeed, transgenic mice lacking iNOS are resistant to LPS-induced cardiovascular alterations and mortality (14, 15).

NO is a free radical species that possesses a reactive unpaired electron (16, 17). It can react rapidly with superoxide (O_2^-) to form a peroxynitrite anion ($OONO^-$) (18). The peroxynitrite anion and peroxynitrous acid are strong oxidizing agents (19), and their decomposition products, $OH^\cdot$ and $NO_2^\cdot$, facilitate lipid peroxidation (18, 19). Since it has been extensively demonstrated that free radical damage and lipid peroxidation are involved in respiratory muscle impairment during sepsis (6, 7, 20), this impairment may be mediated, at least partially, by NO. Two findings support this hypothesis. First, diaphragmatic contractile function can be negatively modulated by NO donors (21). Second, an increase in NOS activity has been reported in the diaphragm of endotoxemic rats (22). However, to our knowledge, no study has documented in the same experimental model of sepsis both diaphragmatic iNOS induction and its consequence on contractile function.

The present study was designed, therefore, to investigate in rats: (*a*) whether iNOS protein was induced in the diaphragm after *Escherichia Coli* endotoxin inoculation; (*b*) the cellular localization of iNOS; and (*c*) the effect of inhibition of NO synthesis and of iNOS induction on diaphragmatic contractile

Address correspondence to Jorge Boczkowski, INSERM U408, Faculté X. Bichat, BP416, 75870 Paris Cedex 18, France. Phone: 331 44856251; FAX: 331 40258818; E-mail: u408@bichat.inserm.fr

Received for publication 1 May 1996 and accepted in revised form 24 July 1996.

J. Clin. Invest.

0021-9738/96/10/1550/10 $2.00
Volume 98, Number 7, October 1996, 1550–1559

1. *Abbreviations used in this paper:* ARDS, adult respiratory distress syndrome; DNMMA, N^G monomethyl D-arginine; Dx, dexamethasone; EDL, extensor digitorium longus; LNMMA, N^G monomethyl L-arginine; NO, nitric oxide; NOS, nitric oxide synthase; i-, e-, and bNOS, inducible, endothelial, and neuronal type nitric oxide synthase.

dysfunction induced by endotoxin. In addition, to investigate whether the diaphragm was selectively affected by LPS, we also investigated iNOS protein expression in the left ventricular myocardium, the abdominal muscles, the intercostal muscles, and the peripheral skeletal muscles soleus and extensor digitorium longus.

Methods

Animals. The present experiments were reviewed and approved by the local Institutional Animal Care and Use Committee and the experimental protocol was in agreement with the recommendations relating to animal studies of the French Law (Ministère des Affaires Sociales et de la Solidarité Nationale, Paris, France). 134 male albino rats of the Sprague Dawley strain (330–360 g) were obtained from Charles River France Inc. (Saint Aubin, Les Elbeuf, France). All rats were housed individually, acclimatized to a 12-h light–dark cycle, and maintained on rat chow (Ralston Purina Co., St. Louis, MO) and tap water ad libitum for a 5-d period before experimental set up. Environmental temperature was 22–23°C during the experimental period.

The animals received two random treatments, intraperitoneally administered: sterile 0.9% sodium chloride solution (C animals) or *E. Coli* endotoxin suspension (1.6 mg/kg body weight, LPS animals). Injection volume was 1.3 ml/kg body wt in both groups. The endotoxin used was lyophilized *E. Coli* LPS (serotype 0.26 B6; Difco Laboratories, Inc., Detroit, MI) that was reconstituted with 0.9% sterile sodium chloride.

LPS animals were randomly divided into three groups according to intravenous administration (tail vein) of (*a*) sterile 0.9% sodium chloride solution (group LPS, $n = 61$); (*b*) N^G monomethyl L-arginine (LNMMA), a potent and specific inhibitor of NOS activity in vitro and in vivo (see reference 23 for review), (group LPS+LNMMA, $n = 11$); or (*c*) dexamethasone (Dx), which blocks iNOS induction (24, 25), (group LPS+Dx, $n = 16$). Sterile 0.9% sodium chloride solution was administered 90 min after sodium chloride or LPS administration. LNMMA was administered at a dose of 8 mg/kg, 90 min after sodium chloride or LPS administration. Dexamethasone was administered at a dose of 4 mg/kg, 45 min before sodium chloride or LPS administration. Injection volume was 1.3 ml/kg body wt in the three cases.

C animals received intravenously (tail vein) sterile 0.9% sodium chloride solution (1.3 ml/kg body wt) 90 min after intraperitoneal sodium chloride (C group, $n = 20$). In previous experiments, we verified that administration of LNMMA and dexamethasone to C animals did not modify the biochemical and contractile properties evaluated in the present study.

To evaluate the specificity of the effect of LNMMA, another group of animals received LPS plus N^G monomethyl D-arginine (DNMMA; group LPS+DNMMA, $n = 6$), a stereoisomer of LNMMA that did not inhibit NO synthesis (23). DNMMA was administered at the same dose and time as LNMMA.

Animals of group LPS were killed 2, 6, 12, 24, and 48 h after LPS administration ($n = 6$, 8, 16, 22, and 9, respectively). The other groups of LPS animals (LPS+LNMMA, LPS+DNMMA and LPS+Dx) and animals of group C were killed only 24 h after LPS or sodium chloride inoculation. In previous experiments, we verified that biochemical and diaphragmatic contractile parameters from animals of the group C were similar at the different time points of the study. At these times, animals were anesthetized with sodium pentobarbital (50 mg/kg body wt i.p.). The thoracic and abdominal cavities were opened immediately, and the animals were exsanguinated via the abdominal aorta. The diaphragm with its origins and insertion on the ribs and central tendon left intact was quickly excised and transferred to a dissecting dish containing oxygenated Kreb's solution (composition [in mM]: 137 NaCl, 4 KCl, 1 $MgCl_2$, 1 KH_2PO_4, 12 $NaHCO_3$, 2 $CaCl_2$, and 6.5 glucose) into which it was pinned to maintain resting length during dissection. The solution was bubbled with a mixture of 95% O_2/5% CO_2. Temperature and pH were controlled (37°C and 7.40, respectively) and were monitored continuously. Krebs solution was exchanged frequently. Muscular samples from the lateral costal region of each hemidiaphragm were dissected. This region was chosen because it was shown to contain parallel fiber layers and to be composed by equally distributed fiber types (26). One sample was carefully prepared for the study of contractile properties. Another sample was mounted for immunohistochemistry and histologic examination (these examinations were performed in groups C and LPS). Another sample weighed immediately after death (wet weight) and after a 72-h desiccation (dry weight). Finally, other samples were freeze-clamped separately and stored at −80°C until use for biochemical assays.

A subset of animals of groups C and LPS ($n = 5$ and 15, respectively) was killed 24 h after sodium chloride or LPS administration and samples from the left ventricular myocardium, the intercostal muscles, the abdominal muscles, and the peripheral skeletal muscles soleus and extensor digitorium longus (EDL) were dissected, in addition to the diaphragm. The animals were anesthetized with sodium pentobarbital (50 mg/kg body wt i.p.). Peripheral muscles were dissected first, and then samples from the abdominal muscles, the diaphragm, the left ventricular myocardium, and the intercostal muscles were dissected, as described previously. These samples were freeze-clamped separately and stored at −80°C until use for biochemical assays.

Biochemical assays. For all the biochemical assays, frozen muscle samples (50–100 mg) were homogenized by an Ultraturrax T25 (Janke and Kunkel; IKA Works, Inc., Cincinnati, OH).

Western blot analysis. Tissue samples were homogenized in 0.3 ml lysis buffer (50 mM Tris-HCl, pH 7.4, 0.1 mM EDTA, 1 μM leupeptin, 1 μM PMSF, 1 μM Aprotinin). Proteins (150 and 300 μg per lane for the diaphragm and the left ventricular myocardium, respectively) in the tissue homogenates were denatured by boiling for 5 min in sample buffer (0.5 M Tris-HCl, pH 6.8, 10% [wt/vol] SDS, 10% [vol/vol] glycerol, 5% [vol/vol] 2-b-mercaptoethanol, 0.05% [wt/vol] bromophenol blue) and separated by electrophoresis on precasted 7.5% SDS–polyalcrylamide gel (Bio-Rad Laboratories, Richmond, CA). They were transferred overnight at 4°C to a nylon membrane (Zeta-Probe® GT; Bio-Rad Laboratories) in 25 mM CAPSO (3-[Cyclohexylamino]-2-hydroxy-1-propanesulfonic acid) buffer (pH 10) and 20% methanol. Subsequent steps were performed at room temperature. The membranes were then blocked with 10% nonfat dry milk in Tris-buffered saline (25 mM Tris, pH 7.5, 150 mM NaCl) + 0.05% (vol/vol) Tween 20 (TBST solution). After washing in TBST, the membranes were incubated 1 h with a rabbit antimurine iNOS polyclonal antibody (Transduction Laboratories, Lexington, KY) used at a 1:250 dilution. This antibody was raised against a 21-kD protein fragment corresponding to peptide sequence 961–1144 of mouse iNOS and was affinity purified on a column of the respective immunogen coupled to agarose. After washing, the membranes were incubated for 1 h with a 1:3,000 dilution of a goat anti–rabbit IgG conjugated to alkaline phosphatase (Bio-Rad Laboratories). The blots were washed with TBST, followed by detection of immunoreactive proteins by the enhanced chemiluminescence method using AMMPD® (Tropix, Inc., Bedford, MA) as a substrate.

A lysate of *E. Coli* LPS-stimulated (10 μg/ml) rat alveolar macrophages obtained by lavage was used as a positive control for detection of iNOS protein. The lysate was prepared as previously reported (27). After a 24-h incubation period, the supernatant was removed and the cells were scraped in lysis buffer (500 μl/10^6 cells). Alveolar macrophage proteins (< 10 μg per well) were denatured by boiling for 5 min in sample buffer.

Inducible nitric oxide synthase activity measurement. Muscle samples were homogenized in 1 ml lysis buffer solution. Nitric oxide synthase activity was measured by the conversion of [^{3}H]L-arginine to [^{3}H]L-citrulline according to the method described by Bredt and Snyder (28) in the absence of calcium and calmodulin in the reaction buffer, to selectively assess the activity of iNOS (29). Briefly, 25 μl tissue homogenate, corresponding to 50 μg total cellular protein, were incubated for 60 min at 37°C in the reaction buffer containing 50 mM

Hepes (pH 7.40), 0.5 mM NADPH, 5 μM FAD, and 5 mM tetrahydrobiopterin (B. Schirks Laboratories) and 50 nM of [^{3}H]L-arginine (specific activity, 35.7 Ci/mmol) in a total volume of 150 μl. The enzymatic reaction was halted by the addition of 2 ml ice-cold 20 mM Hepes (pH 5.5)/2 mM EDTA, and the total volume was applied to a Dowex-50W X8 column (Bio-Rad Laboratories) preequilibrated with the same buffer. [^{3}H]L-arginine was retained on the column, whereas [^{3}H]L-citrulline was eluted with 2 ml of deionized water and its concentration was determined by liquid scintillation counting. Initial experiments showed that the reaction was linear for 60 min, and that it was concentration-dependently inhibited by the addition of LNMMA to the reaction buffer. Indeed, inhibition of iNOS activity, expressed as a percentage of the untreated sample, was 4.1±1.5; 55.2±0.7, and 94.6±2.7 with 100 nM, 10 μM, and 1 mM of LNMMA, respectively (n = 4 for each concentration of LNMMA).

Cyclic GMP assay. Muscular samples were homogenized in 1 ml/100 mg tissue of 6% (wt/vol) ice-cold trichloroacetic acid. After centrifugation at 10,000 g at 4°C for 15 min, the supernatants were collected and trichloroacetic acid was extracted by washing the supernatants four times with 5 vol water-saturated ether. The remaining ether was evaporated overnight and the samples were lyophilized. Cyclic GMP content was determined by enzyme immunoassay (Amersham International, Little Chalfont, UK) by acetylating the samples before the assay. With this technique, cyclic GMP can be measured in the range of 2–512 fmol/well (0.7–176 pg/well). Cross-reactivity of cyclic GMP with anti–cAMP antibody was 0.00016%.

Muscular protein concentration. Protein concentration was measured spectrophotometrically in 96-well plates using the Bio-Rad protein reagent (Bio-Rad Laboratories), with bovine serum albumin as standard.

Immunohistochemistry and histologic examination. Muscle strips obtained from the costal region of the diaphragm were put into tissue glue (PolyFreeze™; Polysciences Inc., Warrington, PA) on a cork holder, with the muscle fibers oriented perpendicularly to the surface of the cork. Subsequently, these specimens were quickly frozen in isopentane cooled with liquid N_2. Serial sections (10-μm thick) were cut with a cryostat after the samples were warmed to −20°C. For immunohistochemistry, the sections were allowed to dry overnight and subsequently fixed in acetone for 5 min. Then they were rinsed in PBS and incubated in blocking buffer (PBS containing 1% bovine serum albumin and 2% normal goat serum) for 1 h at room temperature. After this, the slides were incubated with the same rabbit anti–iNOS antibody used for the Western blot (Transduction Laboratories). Incubation was effectuated during 1 h at room temperature and the concentration of the antiserum was 0.5 μg/ml. The slides were washed in PBS and successively exposed to a biotinylated goat antiserum to rabbit immunoglobulin G (Dako Corp., Carpinteria, CA) diluted 1:500, and a complex of streptavidin–biotin–alkaline phosphatase (Dako Corp.). Localization of phosphatase alkaline was revealed by using the Fast Red substrate solution (Dako Corp.). The specificity of the immunostaining was studied by omission of the primary antibody, as well as by using pooled nonimmune rabbit IgG instead of the primary antibody at equivalent protein concentration and processed as above.

Quantification of immunostaining was performed using a Perfect Image™ 2.01 image analysis system (ICONIX, Courtaboeuf, France). Digitized images of five randomly selected fields of three nonserial sections from each diaphragmatic sample were segmented by interactive thresholding to separate immunostaining from background. The area of diaphragmatic myocytes immunostaining was expressed as a percentage of the field area. Analysis of the images was performed independently by J. Boczkowski and G. Danialou. Concordance in the analysis was observed in 91% of the cases. In the remaining cases, analysis was performed simultaneously and a common conclusion was attempted. For histologic examination, tissue sections were stained with hematoxylin and eosin.

Contractile function. A bundle from the middle part of the lateral costal region of the diaphragm (∼ 2 mm wide) was microscopically dissected with fibers attached to a portion of the ribs and distally to the central tendon. The tendinous end was left intact while the other end was cut free of the ribs and ligated with fine copper wire (20 μm diameter) for use in mounting the preparation.

The bundles (19.4–20.3 mg) were mounted horizontally into an open-topped Plexiglas tissue chamber. They were immobilized by snaring the tendon, with fine surgical silk, into one end of the channel and connecting the other extremity of the bundle, by means of a 20-μm copper wire, to the tip of the force transducer. The experimental chamber and force transducer were mounted on an antivibration table (Harvard Apparatus, Inc., South Natick, MA).

The preparations were perfused with continually flowing Kreb's solution, which prevented alterations in salinity and allowed rapid elimination of toxic metabolites released from the muscles. As stated previously, the solution was bubbled with a mixture of 95% O_2, 5% CO_2, and the temperature and pH were controlled (37°C and 7.40, respectively) and monitored continuously during the experiment.

The bundles were electrically stimulated by means of rectangular platinum field electrodes mounted on both sides of the channel parallel to the tissue strip. Stimuli of 0.5-ms duration were applied using an S 48 Stimulator (Grass Instrument Co., Quincy, MA) connected in series with a power amplifier (Grass Instrument Co.). Stimulus intensity was increased until maximal twitch tension responses were obtained, and then set at 1.2 × the maximal to ensure supramaximal stimulation (near 30 V).

Isometric force was measured with an FT 03 force transducer (Grass Instrument Co.), mounted on a micrometer that allowed adjustment of the preparation to optimal length, which is the length at which peak twitch force was maximal. The signal from the force transducer was amplified and displayed simultaneously on a TA550 paper recorder (Gould Inc., Cleveland, OH) and an N 5111 storage oscilloscope (Tektronix Inc., Beaverton, OR).

Peak twitch force was measured from a series of contractions induced by single-pulse stimuli. The force–frequency relationship was studied using 1-s–duration trains of stimuli at 10, 20, 30, 50, 100, and 120 Hz. At least 1 min intervened between each stimulus train. Force, expressed in Newtons, was normalized for muscle cross-sectional area, which was estimated by dividing bundle weight by length and specific density (1.056 g/cm^3, reference 30).

Fatigability was assessed by means of 300-ms stimulations at 30 Hz and applied every second for 3 min (modified from reference 31). Fatigability was quantified with two indexes: (*a*) the ratio of force generated after 3 min of stimulation to the initial force, and (*b*) the time to decrease to a half of the initial force.

Reagents. LNMMA, DNMMA, EDTA, EGTA, DTT, leupeptin, PMSF, Hepes, NADPH, FAD, calmodulin, Tris, Tween 20, and CAPSO were obtained from Sigma Chemical Co. (La Verpillière, France). Dexamethasone was supplied by Merck Sharp & Dohme Chibret Products, (Nogent sur Marne, France). [^{3}H]L-arginine was from DuPont-NEN (Boston, MA). Tetrahydrobiopterin was supplied by Research Biomedical Inc. (Natick, MA). SDS, glycerol, 2-b-mercaptoethanol, and bromophenol blue were obtained from Bio-Rad Laboratories. Alveolar macrophages culture media, supplements, and fetal bovine serum were from Flow Laboratories (Irvine, Ayrshire, Scotland). Tissue culture plasticware was supplied by Costar Corp. (Cambridge, MA).

Statistical analysis. Values are given as mean±SEM. The data obtained for the different groups were analyzed by ANOVA. When the F value was significant ($P < 0.05$), we performed a post-hoc analysis with the Duncan new multiple range test to test the differences between means (32). Significance for all statistics was accepted at $P < 0.05$.

Results

Effects of endotoxin on the diaphragm

Diaphragmatic iNOS protein induction. Whole diaphragm homogenates from LPS-inoculated animals reproducibly ex-

pressed iNOS protein as detected by Western blot, with a molecular weight identical to iNOS protein expressed by in vitro LPS-stimulated rat alveolar macrophages (Fig. 1, *A*, lanes *c–e*, and *j*). Indeed, iNOS protein could be reproducibly detected as early as 6 h after LPS inoculation and persisted for up to 24 h. No iNOS protein could be detected 2 or 48 h after LPS inoculation (lanes *b* and *f*, respectively). No iNOS protein could be detected in whole diaphragm homogenates obtained from control animals or in cell homogenates of rat alveolar macrophages not exposed in vitro to LPS (lanes *a* and *i*, respectively).

Induction of diaphragmatic iNOS activity, measured by the conversion of [^{3}H]L-arginine to [^{3}H]L-citrulline in the absence of calcium and calmodulin in the reaction buffer, paralleled induction of iNOS protein (Fig. 1 *B*). Indeed, [^{3}H]L-citrulline formation from [^{3}H]l-arginine was significantly and similarly increased 6, 12, and 24 h after LPS inoculation in comparison to the low basal levels observed in control animals ($P < 0.001$). 2 and 48 h after LPS inoculation, [^{3}H]L-citrulline formation from [^{3}H]L-arginine was not different from that of control animals.

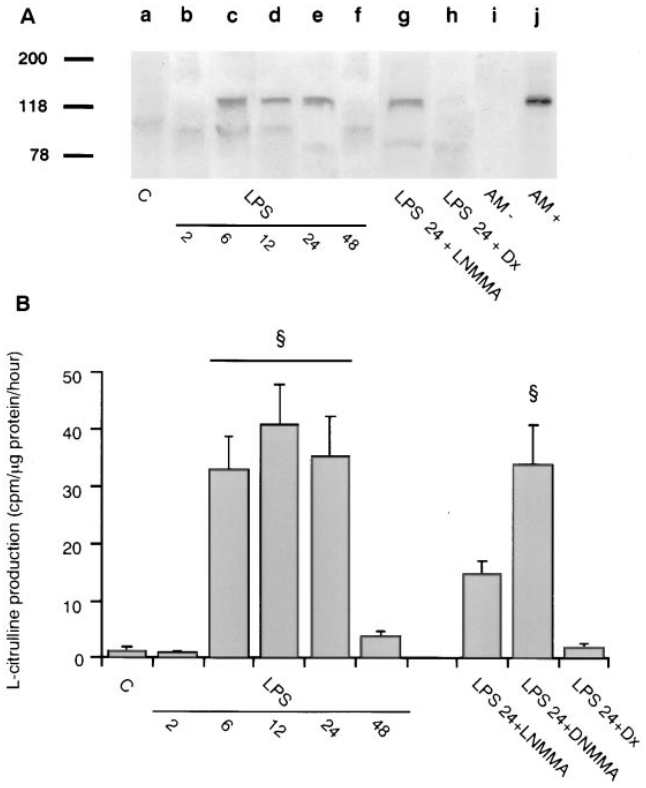

Figure 1. (*A*) Representative Western analysis of iNOS protein in the rat diaphragm. Proteins from diaphragmatic homogenates from a control animal (*C*, lane *a*), from animals killed 2, 6, 12, 24, and 48 h after endotoxin inoculation (*LPS 2*, *6*, *12*, *24*, and *48*, lanes *b–f*, respectively), from animals killed 24 h after endotoxin inoculation and that received LNMMA or dexamethasone (LPS 24+LNMMA and LPS 24+Dx, lanes *g* and *h*, respectively), and from rat alveolar macrophages nonstimulated and stimulated with LPS (AM- and AM+, lanes *i* and *j*, respectively) were separated by 7.5% SDS-PAGE and transferred to a nylon membrane. Immunoblot was performed as described in Methods. Molecular size markers in kilodaltons are shown on the left. A main band with an estimated molecular weight of 130 corresponding to iNOS is present in samples from the diaphragm of the LPS 6, 12, 24, and 24+LNMMA animals and from the LPS-stimulated rat alveolar macrophages. By contrast, no band is present in the diaphragms from the control, LPS 2, 48, LPS 24+Dx animals, and from the nonstimulated rat alveolar macrophages. (*B*) Diaphragmatic iNOS activity in the different groups of animals. iNOS activity was expressed as counts per minute/microgram protein of [^{3}H]L-citrulline and by minutes of incubation. Each bar represents the mean±SEM of each group. $^{\S}P < 0.001$ vs group C.

Diaphragmatic cyclic GMP content. Cyclic GMP content of diaphragm homogenates was low in group C and it increased significantly in group LPS. However, the time course of this increase was different from iNOS protein and enzymatic activity. In fact, maximal increase in cyclic GMP was reached at 6 h and sustained for up to 48 h (Fig. 2, $P < 0.05$ for group LPS at 6, 12, 24, and 48 h vs group C). 2 h after LPS inoculation, cyclic GMP content was similar to that in group C.

Diaphragmatic dry-to-wet weight ratio, histology, and immunohistochemistry. Diaphragmatic dry-to-wet weight ratio was similar in C and LPS groups. In fact, diaphragmatic dry-to-wet weight ratio was 0.29±0.01 in C animals and 0.29±0.01, 0.29±0.02, 0.29±0.01, 0.29±0.01, and 0.29±0.02 in LPS animals 2, 6, 12, 24, and 48 h after endotoxin administration, respectively. Histologic analysis of the diaphragm in group LPS showed no alteration of muscular fibers and an absence of tissue oedema during the whole duration of the experimental period (Fig. 3). By contrast, 6 h after LPS inoculation, clusters of inflammatory cells were present adhering to the wall of postcapillary venules and infiltrating the perivascular space (Fig. 3). These cells were still present but very few in number at 12 h and they disappeared 24 h after LPS inoculation.

An increased iNOS staining was observed in the diaphragm of LPS animals. This staining was present in different cell types depending on the time point considered. 6 and 12 h after LPS inoculation, staining was constantly observed in the inflammatory cells (Figs. 4 and 5). 12 and 24 h after LPS, iNOS staining was reproducibly observed in diaphragmatic myocytes in a diffuse cytoplasmic pattern occupying a variable portion of the myocyte surface (Fig. 5). All of the sections of each sample from LPS 12 and 24 animals showed iNOS staining. In both groups of animals, quantification of the immunostaining

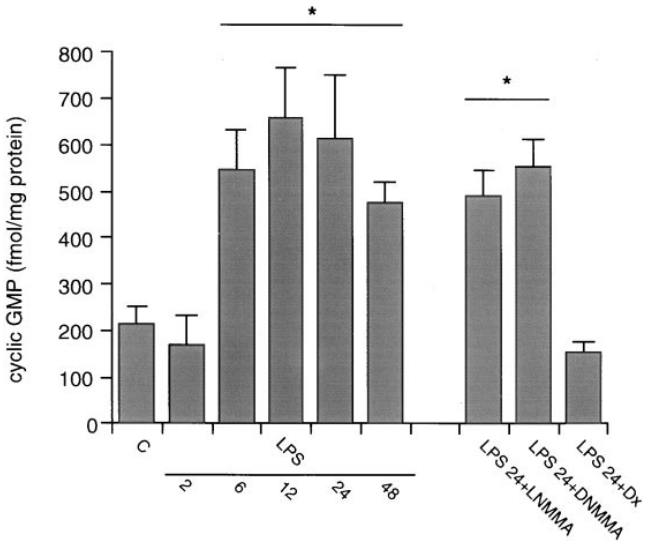

Figure 2. Diaphragmatic cyclic GMP content in the different groups of animals. Each bar represents the mean±SEM of each group. $^{*}P < 0.05$ vs group C.

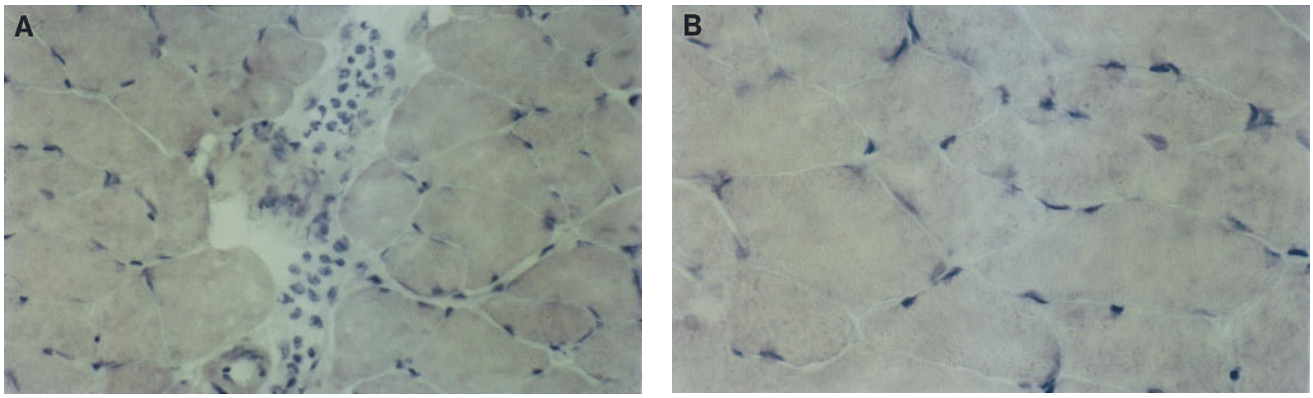

Figure 3. Histologic analysis of the diaphragm. In group LPS, no alteration of muscular fibers and or tissue oedema was observed at 6 or 24 h (*A* and *B*). Similar data were noted at the other time points of the study. 6 h after LPS inoculation, clusters of polymorphonuclear and mononuclear cells were present, infiltrating the perivascular space (*A*). These cells disappeared 24 h after LPS inoculation (*B*). ×250 (*A*) and ×400 (*B*).

showed that the area of diaphragmatic myocytes iNOS staining was similar, reaching 40.2±3.4% and 45.2±3.8% of the field area respectively. By contrast, no sample from C or LPS animals killed 2, 6, and 48 h after inoculation showed iNOS staining in diaphragmatic myocytes (Fig. 5). No iNOS staining was observed when the anti–iNOS antiserum was omitted (Fig. 4). No tissue section showed positive immunostaining with nonimmune serum (data not shown).

Diaphragmatic force. No difference was observed in diaphragmatic bundles dimensions among the different groups of animals. Values of diaphragmatic bundles length were comprised between 14.5 and 16.2 mm in the different experimental groups.

Diaphragmatic force was significantly reduced in LPS animals only at 12 and 24 h. Indeed, 12 and 24 h after LPS inoculation, diaphragmatic peak twitch and maximal tetanic tension (tension observed at 120-Hz stimulation) were significantly lower in group LPS than in group C ($P < 0.0001$; Fig. 6). Analysis of diaphragmatic force–frequency relationship showed that force generated in response to all stimulation frequencies

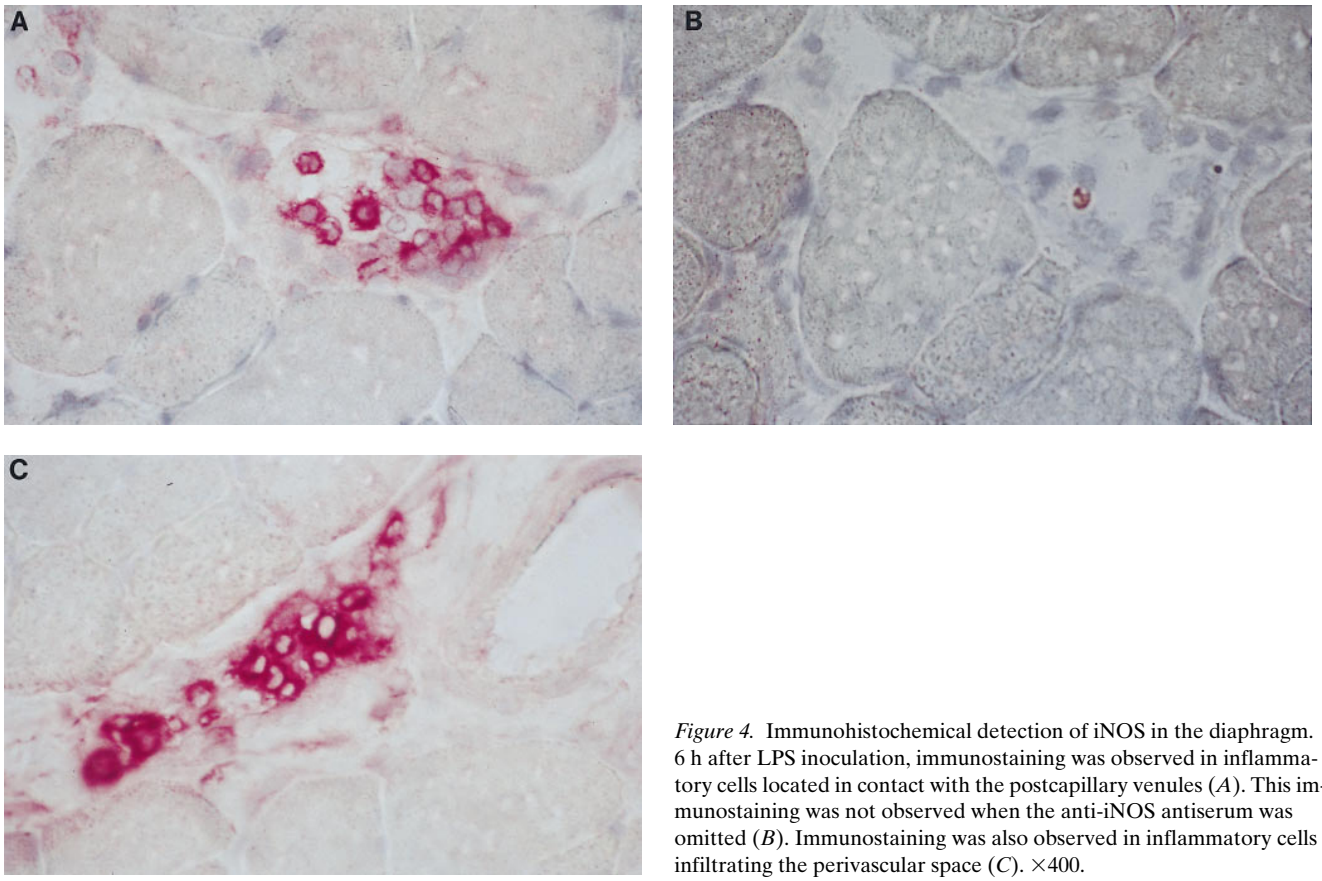

Figure 4. Immunohistochemical detection of iNOS in the diaphragm. 6 h after LPS inoculation, immunostaining was observed in inflammatory cells located in contact with the postcapillary venules (*A*). This immunostaining was not observed when the anti-iNOS antiserum was omitted (*B*). Immunostaining was also observed in inflammatory cells infiltrating the perivascular space (*C*). ×400.

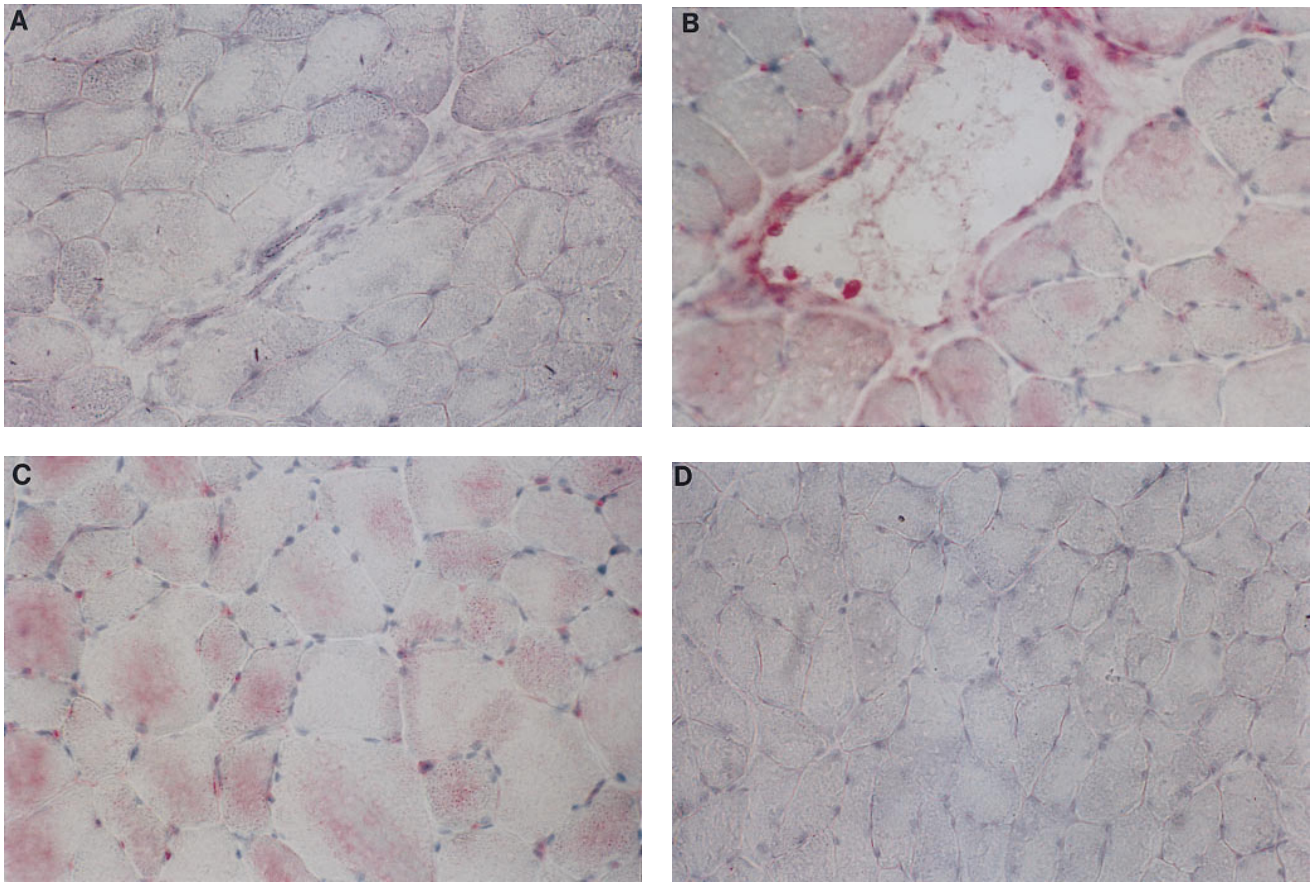

Figure 5. Immunohistochemical detection of iNOS in the diaphragm. 12 and 24 h after LPS inoculation, iNOS staining was observed in diaphragmatic skeletal myocytes (*B* and *C*). At 12 h, immunostaining was also observed in some inflammatory cells located in contact with the wall of a venule and in the perivascular space. A comparable section from a control animal and from an animal killed 48 h after LPS showed no immunoreactivity (*A* and *D*). ×400.

was lower in group LPS than in group C at these time points (data not shown). Diaphragmatic peak twitch tension was similar 12 and 24 h after LPS. In contrast, maximal tetanic tension was significantly lower after 24 than 12 h of LPS ($P < 0.05$).

Diaphragmatic fatigability was not modified by endotoxin inoculation. The ratio of force generated after 3 min of stimulation to the initial force and the time to decrease to half the initial force were not different in C than in LPS animals, and this whatever the time point considered (Table I).

Effects of LNMMA and dexamethasone on diaphragmatic alterations induced by endotoxin

Effects of LNMMA. Administration of LNMMA 90 min after endotoxin suppressed the induction of diaphragmatic iNOS activity observed 24 h after endotoxin, whereas the induction of iNOS protein was not modified. iNOS activity was significantly reduced in group LPS+LNMMA as compared to group LPS 24 h after inoculation ($P < 0.005$), whereas it was not different from group C (Fig. 1 *B*). By contrast, Western blotting identified an iNOS protein band in samples from LPS+LNMMA animals (Fig. 1 *A*, lane *g*). Diaphragmatic cyclic GMP content was not modified in group LPS+LNMMA as compared to group LPS (Fig. 2). The decrease in diaphragmatic force induced by LPS 24 h after inoculation was not observed after LNMMA administration. Peak twitch and maximal tetanic tension were significantly higher in group LPS+LNMMA than in group LPS ($P < 0.05$), but not different from group C (Fig. 6). Identical results were obtained for all the frequencies of stimulation (data not shown). Administration of LNMMA to LPS animals did not modify diaphragmatic fatigability (Table I).

When DNMMA was administered instead of LNMMA, no further modification of the effect of endotoxin was observed. Diaphragmatic iNOS activity and force were similar in group LPS+DNMMA and in group LPS, but significantly different from group C. Indeed iNOS activity was significantly higher and force was significantly lower in group LPS+DNMMA than in group C (group LPS+DNMMA vs group C: $P < 0.05$ for iNOS activity, and $P < 0.0001$ for the force for all the frequencies of stimulation; Figs. 1 *B* and 6, respectively).

Effects of dexamethasone. Administration of dexamethasone before LPS prevented diaphragmatic iNOS protein induction. Consequently, in LPS+Dx animals, no iNOS protein was detected (Fig. 1 *A*, lane *h*) and iNOS activity was significantly lower than in group LPS ($P < 0.01$), being not different from group C (Fig. 1 *B*). The same result was observed concerning cyclic GMP content (Fig. 2). Consistent with these results, diaphragmatic peak twitch and maximal tetanic force were significantly higher in group LPS+Dx than in group LPS, whereas they were not different from group C ($P < 0.0001$

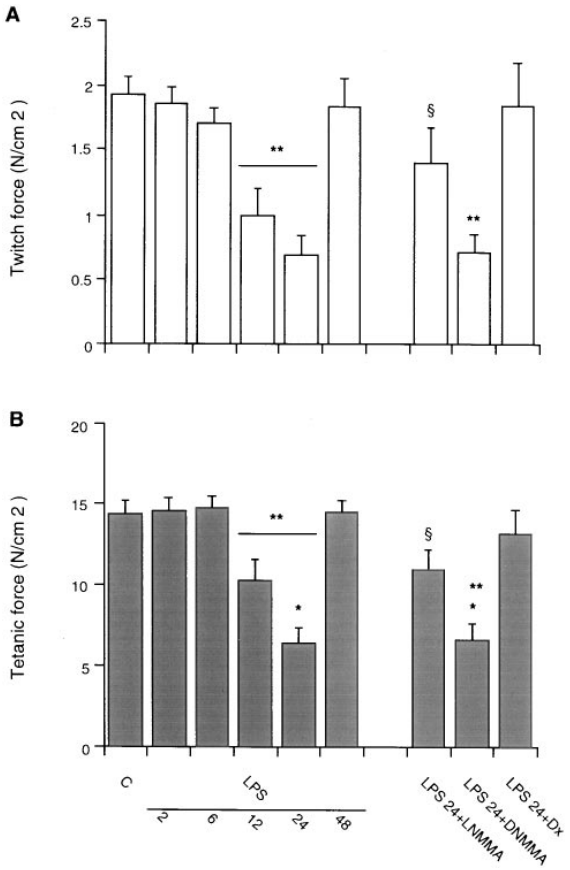

Figure 6. Diaphragmatic twitch force (*A*) and tetanic force (*B*) in the different groups of animals, expressed in N/cm^2. Each bar represents the mean±SEM of each group. $^{**}P < 0.0001$ vs C, $^{*}P < 0.05$ vs LPS 12, and $^{\S}P < 0.05$ vs LPS 24. N, Newton.

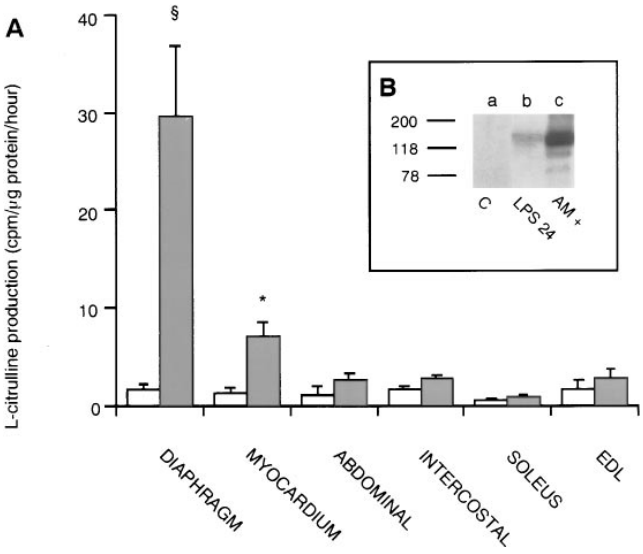

Figure 7. (*A*) iNOS activity in the diaphragm and in nondiaphragmatic muscles. iNOS activity was expressed as counts per minute/microgram protein of [^{3}H]L-citrulline and by minutes of incubation. Each bar represents the mean±SEM of each group. $^{\S}P < 0.001$ vs C, and $^{*}P < 0.05$ vs C and vs the diaphragm. (*B*) Representative Western blot analysis of iNOS protein in the rat heart. Proteins from heart homogenates from a control animal (*C*, lane *a*), from an LPS animal killed 24 h after LPS inoculation (*LPS 24*, lane *b*), and from LPS stimulated rat alveolar macrophages (*AM+*, lane *c*) were separated by 7.5% SDS-PAGE and transferred to a nylon membrane. Immunoblot was performed as described in Methods. Molecular size markers in kilodaltons are shown on the left. A main band with an estimated molecular weight of 130 kD is observed in the samples from the LPS 24 heart and from the stimulated alveolar macrophages.

group LPS+Dx vs group LPS, and NS vs group C; Fig. 6). The same result was observed for all the frequencies of stimulation (data not shown). Administration of dexamethasone to LPS animals did not modify diaphragmatic fatigability (Table I).

Table I. Diaphragmatic Fatigability in the Different Groups of Animals

Group	Half time	Force
	s	*final/initial*
C	62.8±14.8	19.1±4.5
LPS 2	61.3±17.3	17.9±4.7
LPS 6	58.7±23.9	16.9±6.9
LPS 12	60.2±24.6	18.4±7.5
LPS 24	65.2±19.7	20.7±6.2
LPS 48	50.9±17.0	12.9±4.3
LPS 24+LNMMA	53.7±19.0	17.3±6.1
LPS 24+DNMMA	60.7±21.3	19.3±5.7
LPS 24+Dx	59.8±16.6	19.1±5.3

Half time: time to decrease to half the initial force. Force (final/initial): ratio of force generated after 3 min of stimulation to the initial force. There was no difference between C and LPS animals at each time point considered. Values are mean±SEM.

Induction of iNOS protein in the diaphragm and in nondiaphragmatic muscles

24 h after endotoxin administration, an increase in iNOS activity was detected only in samples from the diaphragm and from the left ventricular myocardium (Fig. 7 *A*). However, this increase was significantly smaller in the myocardium than in the diaphragm ($P < 0.05$). No significant increase in iNOS activity was observed in LPS animals in the samples from the intercostal muscles, the abdominal muscles, and the peripheral skeletal muscles soleus and EDL. In LPS animals, Western blot identified a main iNOS protein band in the left ventricular myocardium (Fig. 7 *B*, lane *b*). This band was absent in samples from C animals. No iNOS band was observed in LPS animals in the samples from the intercostal muscles, the abdominal muscles, and the peripheral skeletal muscles soleus and EDL (data not shown).

Discussion

The main results of this study are: (*a*) iNOS protein was induced in the rat diaphragm after *E. Coli* endotoxin inoculation; (*b*) iNOS was first present in clusters of inflammatory cells infiltrating the perivascular spaces of the muscle, and then in diaphragmatic fibers; (*c*) iNOS induction in diaphragmatic fibers was associated with a decreased muscular force; (*d*) inhibition of NO synthesis with LNMMA or of iNOS induction with dexamethasone prevented the decrease in diaphragmatic

force induced by endotoxin; and (*e*) diaphragmatic iNOS induction in the present experimental model was not part of a common response of skeletal musculature to endotoxin. Indeed, in LPS animals no iNOS induction was observed in the intercostal, abdominal, or peripheral muscles soleus or EDL. By contrast, iNOS protein was induced in the left ventricular myocardium. To our knowledge, these data demonstrate for the first time in vivo iNOS induction in diaphragmatic myocytes and its involvement in the genesis of diaphragmatic contractile dysfunction after *E. Coli* endotoxin inoculation.

The increase in diaphragmatic iNOS activity that we observed in LPS rats agrees with data reported by Salter et al. (22) who found an increase in NOS activity in the rat diaphragm 6 h after inoculation of *Salmonella Typhimurium* LPS. The time course study we performed showed that induction of iNOS protein in the whole diaphragm was maximal 6 h after LPS and sustained for up to 24 h. However, examination of the cellular types in which iNOS was induced showed a biphasic time course response with an early induction (6 h) in clusters of inflammatory cells located in contact with the diaphragmatic venules and infiltrating the perivascular space, and a late induction (12 and 24 h) in skeletal myocytes. Whereas kinetics of iNOS expression has been abundantly studied in vitro in neonatal and adult skeletal and cardiac myocytes (33–36), no data are available in the current literature that allow us to compare the present results with others performed in vivo in the skeletal musculature. However, the time course we found agrees with previous data reported in vitro by Williams et al. (33). These authors compared nitrite production by the C_2C1_2 mouse skeletal muscle myocytes vs the RAW macrophages exposed to the same cytokine mix containing components necessary for maximal stimulation of each cell type. The total nitrite produced by myocytes and macrophages was indistinguishable at 24 h after stimulation. However, nitrite accumulation occurred significantly faster in macrophages than in myocytes. In fact, nitrite production by the RAW macrophages was first detected at 6 h of stimulation, as opposed to myocytes in which nitrite accumulation was only significant from 12–16 h.

The elevation of cyclic GMP observed in diaphragmatic muscle 24 h after LPS inoculation was not related to iNOS induction. Indeed, diaphragmatic cyclic GMP was similar in both LPS and LPS+LNMMA groups. Furthermore, cyclic GMP content remained elevated 48 h after LPS, a time point where iNOS protein expression was undetectable. These results are surprising since it is largely known that NO activates the soluble guanylyl cyclase to synthetize cyclic GMP (12). To further evaluate the role of iNOS induction on cyclic GMP synthesis, we measured diaphragmatic cyclic GMP concentration in a subgroup of LPS+LNMMA animals killed 6 h after LPS inoculation. In these animals ($n = 6$) cyclic GMP concentration was 262.8±162.1 fmol/mg protein, a value that was similar to the group C. This result showed that activation of soluble guanylyl cyclase, in the present experimental protocol of LPS inoculation, followed a biphasic time course profile. Early activation of soluble guanylyl cyclase appeared to be due to NO synthetized by iNOS, and late activation was independent of NO. Identification of the factor(s) involved in activation of guanylyl cyclase other than NO is beyond the aim of the present study. However, it is noteworthy that IL-1 (37), oxygen free radicals (38), and products of the phospholipase A_2 such as arachidonic acid (39) have been shown to activate soluble guanylyl cyclase. The fact that dexamethasone abolished the late NO-independent increase in diaphragmatic cyclic GMP supports the implication of IL-1 or arachidonic acid since the synthesis of both molecules is inhibited by glucocorticoids (40, 41).

Comparison of the diaphragm with the other skeletal muscles showed that the diaphragm was particularly susceptible to endotoxin, at least concerning iNOS induction. The absence of iNOS induction in peripheral skeletal muscles agrees with data previously reported by Salter et al. (22) in rats after a 4-h endotoxemic period. The particular susceptibility of the diaphragm could be related to the high blood flow that reaches this muscle during endotoxemia (42). Indeed, a high blood flow could vehiculize more inflammatory cells to the diaphragm than to the peripheral skeletal muscles, and these cells could in turn release locally inflammatory mediators responsible for iNOS induction (29). However, this hypothesis seems improbable because no iNOS induction was detected in the intercostal muscles, in which blood flow is also elevated during endotoxemia (42). Alternatively, selective iNOS induction in the diaphragm may be related to a local effect of the intraperitonealy administered LPS on the muscle. In fact, although it has been shown that LPS is absorbed into the blood after intraperitoneal administration (43), inducing systemic inflammatory changes such as an increase in nitrites and nitrates in plasma (44) and a concomitant induction of iNOS in different organs (45, 46) as observed here in the myocardium, the direct exposition of the diaphragm to LPS could be involved, at least in part, in muscular iNOS induction. However, the absence of iNOS induction in the abdominal muscles, which were also directly exposed to the intraperitonealy administered LPS, does not support this hypothesis. Nevertheless, an effect of LPS on the diaphragm via the peritoneum cannot be completely ruled out because the action of the respiratory muscles draws fluid within the abdominal cavity to the undersurface of the diaphragm, thus overexposing this muscle to LPS as compared with the abdominal muscles.

Diaphragmatic force generation was decreased 12 and 24 h after LPS inoculation. Two lines of evidence suggest that this was probably related to an overproduction of NO by iNOS induced in diaphragmatic myocytes. First, the time course of iNOS induction in diaphragmatic myocytes and of the decrease in diaphragmatic force was similar. Second, inhibition of iNOS induction by dexamethasone, and of NO synthesis by LNMMA, prevented the decrease in diaphragmatic force. We are confident that LNMMA significantly inhibited NO synthesis by iNOS in the present study since LNMMA suppressed the increase in diaphragmatic iNOS activity induced by endotoxin. It must be noted that a single bolus of LNMMA, which was administrated 90 min after LPS, significantly inhibited NO synthesis by iNOS 22.5 h later. It is very difficult to compare this result with data published by other authors because, to our knowledge, no study has been reported in the literature using a similar protocol of administration of LNMMA, or describing the in vivo pharmacokinetics of LNMMA or of any of its metabolites. However, two lines of evidence are in agreement with our finding. First, recent studies in rats have shown that N^G-nitro-L-arginine, which is an analogue of L-arginine close to LNMMA, has a half-life of about 20 h and a mean residence time of $\sim$ 25 h (47, 48). Second, several authors demonstrated that LNMMA can behave as a potent mechanism-based irreversible inhibitor of iNOS (49, 50). Therefore, we think that our finding reflects a true long-lasting inhibition of diaphrag-

matic iNOS activity by LNMMA. Furthermore, the absence of effect of DNMMA, a stereoisomer of LNMMA that did not inhibit NO synthesis (23) demonstrated the specificity of the effects of LNMMA. It is interesting to note that in contrast to the decrease in force, diaphragmatic fatigability was not modified in the LPS group. This is a surprising finding because it is generally admitted that respiratory muscle weakness, as found in the present study, predisposes to an increased muscle fatigability (51). However, the effects of endotoxin and sepsis on muscle function are multifactorial and complex (52), and for this reason, results obtained from other causes of muscular weakness cannot necessarily be useful to an understanding of the effects of endotoxin.

Diaphragmatic contractile impairment appeared only when iNOS protein was induced in diaphragmatic myocytes, and not when iNOS was induced in the clusters of inflammatory cells located in diaphragmatic venules and infiltrating the perivascular space of the muscle. This difference could be related to a low level of iNOS induction in the inflammatory cells as compared to myocytes. However, this seems unlikely because iNOS activity in the whole muscle homogenate was similar when iNOS was present only in inflammatory cells (6 h after LPS) and when it was present only in myocytes (24 h after LPS). It must be noted that NO is unique in its ability to diffuse quickly in both aqueous and lipid environments, allowing rapid three-dimensional spread of an NO signal to neighboring tissue elements (53, 54). However, in the present experimental model, NO must be synthetized by the diaphragmatic myocyte itself to impair its force generation. This finding differs from in vitro data showing that NO synthetized by the endothelial cells can depress the contractile function of adjacent heart muscle cells (55).

NO may impair diaphragmatic myocytes contractility through at least four mechanisms. First, NO may change the composition of the muscle fiber bundle; e.g., by inducing swelling, which in turn may decrease force generation in a manner other than by altering contractile protein function. However, we think this mechanism unlikely because diaphragmatic wet-to-dry weight ratio was not different in LPS and C groups. Furthermore, histologic analysis of the diaphragm in group LPS showed no alteration of muscular fibers and an absence of tissue oedema during the whole experimental period. Second, NO may impair diaphragmatic force generation by means of the cyclic GMP signaling pathway. Indeed, it has been recently shown that cyclic GMP can negatively modulate skeletal muscle contractile function (21). However, this seems not to be the case in the present study because the time course of cyclic GMP content and diaphragmatic tension in LPS animals were different. Indeed, 48 h after LPS inoculation, cyclic GMP was still elevated, whereas force was not different from controls. Third, NO may interact with endogenous oxygen free radicals via promotion of peroxynitrite and hydroxyl radicals generation after interaction with O_2^-(18). Since it has been extensively demonstrated that free radical damage and lipid peroxidation are involved in respiratory muscle impairment during sepsis (6, 7, 20), it is conceivable that one mechanism of NO-induced diaphragmatic impairment could be the aggravation of LPS-mediated tissue free radical injury. Finally, a direct deleterious effect of NO on cellular respiration (56, 57) might also contribute to the genesis of its deleterious effect on diaphragmatic contractile function in LPS animals.

In conclusion, this study showed that *E. Coli* endotoxin inoculation in rats induced the expression of iNOS in the diaphragm, and that the NO produced by this enzyme may be involved in the associated impairment of diaphragmatic force generation. Although this study has been performed in animals, it gives new insight in the pathophysiology of diaphragmatic dysfunction observed during sepsis. This may lead to a new therapeutic approach of respiratory failure in which altered respiratory muscle function has been reported.

Acknowledgments

We thank Paul Soler (INSERM U82, Paris, France) and Romain Gherardi (Service dHistologie-Embryologie-Cytogénétique, CHU H. Mondor, Créteil, France) for their helpful advice concerning immunohistochemistry, to Joëlle Benessiano (INSERM U141, Paris, France) for her expert assistance in performing cyclic GMP dosages, and to Bruno Crestani and Claudine Peiffer (INSERM U408) for their encouraging comments. The expert technical assistance of Mrs. Françoise Poron, Christine Zedda, and Corinne Rolland is greatly appreciated.

References

1. Bone, R., R. Balk, F. Cerra, R. Dellinger, A. Fein, W. Knaus, R. Schein, and W. Sibbald. 1992. Definitions for sepsis and organ failure and guidelines for the use of innovative therapies in sepsis. *Chest.* 101:1644–1655.

2. Montgomery, A., M. Stager, C. Carrico, and L. Hudson. 1985. Causes of mortality in patients with the adult respiratory distress syndrome. *Am. Rev. Respir. Dis.* 132:485–489.

3. Hussain, S., G. Simkus, and C. Roussos. 1985. Respiratory muscle fatigue: a cause of ventilatory muscle failure in septic shock. *J. Appl. Physiol.* 58: 2033–2040.

4. Boczkowski, J., B. Dureuil, R. Pariente, and M. Aubier. 1990. Preventive effects of indomethacin on diaphragmatic contractile alterations in endotoxemic rats. *Am. Rev. Respir. Dis.* 142:193–198.

5. Leon, A., J. Boczkowski, B. Dureuil, J. Desmonts, and M. Aubier. 1992. Effects of endotoxic shock on diaphragmatic function in mechanically ventilated rats. *J. Appl. Physiol.* 72:1466–1472.

6. Van Surell, C., J. Boczkowski, C. Pasquier, Y. Du, E. Franzini, and M. Aubier. 1992. Effects of N-acetylcysteine on diaphragmatic function and malondialdehyde content in Escherichia coli endotoxemic rats. *Am. Rev. Respir. Dis.* 146:730–734.

7. Shindoh, C., A. Dimarco, D. Nethery, and G. Supinski. 1992. Effect of PEG-superoxide dismutase on the diaphragmatic response to endotoxin. *Am. Rev. Respir. Dis.* 145:1350–1354.

8. Murciano, D., D. Rigaud, S. Pingleton, M. Armengaud, J. Melchior, and M. Aubier. 1994. Diaphragmatic function in severe malnourished patients with anorexia nervosa: effect of renutrition. *Am. J. Respir. Crit. Care Med.* 150:1569–1576.

9. Davis, J., and L. Loh. 1979. Alveolar hypoventilation and respiratory muscle weakness. *Bull. Eur. Physiopathol. Respir.* 15:45–51.

10. Rochester, D. 1991. Respiratory muscle weakness, pattern of breathing, and CO_2 retention in chronic obstructive pulmonary disease. *Am. Rev. Respir. Dis.* 143:901–903.

11. Cohen, C., G. Zagelbaum, D. Gross, C. Roussos, and P. Macklem. 1982. Clinical manifestations of inspiratory muscle fatigue. *Am. J. Med.* 73:308–316.

12. Moncada, S., and A. Higgs. 1993. The L-arginine–nitric oxide pathway. *N. Engl. J. Med.* 329:2002–2012.

13. Bredt, D., and S. Snyder. 1994. Nitric oxide: a physiologic messenger molecule. *Annu. Rev. Biochem.* 63:175–195.

14. Macmicking, J., C. Nathan, G. Hom, N. Chartrain, D. Fletcher, M. Trumbauer, K. Stevens, Q.-W. Xie, K. Sokol, N. Hutchinson et al. 1995. Altered response to bacterial infection and endotoxic shock in mice lacking inducible nitric oxide synthase. *Cell.* 81:641–650.

15. Wei, X.-Q., I. Charles, A. Smith, J. Ure, G.-J. Feng, F.-P. Huang, D. Xu, W. Muller, S. Moncada, and F. Liew. 1995. Altered immune response in mice lacking inducible nitric oxide synthase. *Nature (Lond.).* 375:408–411.

16. Stamler, J., D. Singel, and J. Loscalzo. 1992. Biochemistry of nitric oxide and its redox-activated forms. *Science (Wash. DC).* 258:1898–1902.

17. Gaston, B., J. Drazen, J. Loscalzo, and J. Stamler. 1994. The biology of nitrogen oxides in the airways. *Am. J. Respir. Crit. Care Med.* 149:538–551.

18. Beckman, J., T. Beckman, J. Chen, P. Marshall, and B. Freeman. 1990. Apparent hydroxyl radical production by peroxynitrite: implications for endothelial injury from nitric oxide and superoxide. *Proc. Natl. Acad. Sci. USA.* 87:1620–1624.

19. Radi, R., J. Beckman, K. Bush, and B. Freeman. 1991. Peroxynitrite-induced membrane lipid peroxidation: the cytotoxic potential of superoxide and nitric oxide. *Arch. Biochem. Biophys.* 288:481–487.

20. Supinski, G., J. Renston, and A. Di Marco. 1992. Free radical mediated diaphragmatic injury following ischemia/reperfusion. *Am. Rev. Respir. Dis.* 145: 672*a.* (Abstr.)

21. Kobzik, L., M. Reid, D. Bredt, and J. Stamler. 1994. Nitric oxide in skeletal muscle. *Nature (Lond.).* 372:546–548.

22. Salter, M., R. Knowles, and S. Moncada. 1991. Widespread tissue distribution, species distribution and changes in activity of $Ca2^{+}$-dependent and $Ca2^{+}$-independent nitric oxide synthases. *FEBS Lett.* 291:145–149.

23. Knowles, R., and S. Moncada. 1994. Nitric oxide synthases in mammals. *Biochem. J.* 298:249–258.

24. Rees, D., S. Cellek, R. Palmer, and S. Moncada. 1990. Dexamethasone prevents the induction by endotoxin of a nitric oxide synthase and the associated effects on vascular tone: an insight into endotoxin shock. *Biochem. Biophys. Res. Commun.* 173:541–547.

25. Geller, D., A. Nussler, M. Di Silvio, C. Lowestein, R. Shapiro, S. Wang, R. Simmons, and T. Billiar. 1994. Cytokines, endotoxin, and glucocorticoids regulate the expression of inducible nitric oxide synthase in hepatocytes. *Proc. Natl. Acad. Sci. USA.* 90:522–526.

26. Metzger, J., K. Scheidt, and R. Fitts. 1985. Histochemical and physiological characteristics of the rat diaphragm. *J. Appl. Physiol.* 58:1085–1091.

27. Crestani, B., P. Cornillet, M. Dehoux, C. Rolland, M. Guenounou, and M. Aubier. 1994. Alveolar type II epithelial cells produce interleukin-6 in vitro and in vivo. Regulation by alveolar macrophage secretory products. *J. Clin. Invest.* 94:731–748.

28. Bredt, D., and S. Snyder. 1990. Isolation of nitric oxide, a calmodulin-requiring enzyme. *Proc. Natl. Acad. Sci. USA.* 87:682–685.

29. Morris, S., and T. Billiar. 1994. New insights into the regulation of inducible nitric oxide synthesis. *Am. J. Physiol.* 266:829–839.

30. Close, R. 1972. Dynamic properties of mammalian skeletal muscles. *Physiol. Rev.* 52:129–197.

31. Burke, R., D. Levine, and F. Zajac. 1971. Mammalian motor units: physiological–histochemical correlation in three types in cat gastrocnemius. *Science (Wash. DC).* 174:709–712.

32. Winer, B. 1971. Statistical principles in experimental design. McGraw-Hill Inc., New York.

33. Williams, G., T. Brown, L. Becker, M. Prager, and B. Giroir. 1994. Cytokine-induced expression of nitric oxide synthase in C2C12 skeletal muscle myocytes. *Am. J. Physiol.* 267:1020–1025.

34. Balligand, J., D. Ungureanu-Longrois, W. Simmons, D. Pimental, T. Malinski, M. Kapturczak, Z. Taha, C. Lowenstein, A. Davidoff, R. Kelly et al. 1994. Cytokine-inducible nitric oxide synthase (iNOS) expression in cardiac myocytes. *J. Biol. Chem.* 269:27580–27588.

35. Tsujimo, M., Y. Hirata, T. Imai, K. Kanno, S. Eguchi, H. Ito, and F. Marumo. 1994. Induction of nitric oxide synthase gene by interleukin-1B in cultured rat cardiocytes. *Circulation.* 90:375–383.

36. Shindo, T., U. Ikeda, F. Ohkawa, Y. Kawahara, M. Yokoama, and K. Shimada. 1995. Nitric oxide synthesis in cardiac myocytes and fibroblasts by inflammatory cytokines. *Cardiovasc. Res.* 29:813–819.

37. Haglund, U., and B. Gerdin. 1991. Oxygen free radicals (OFR) and circulatory shock. *Circ. Shock.* 34:405–411.

38. DeWitt, D. 1991. Prostaglandin endoperoxide synthase: regulation of enzyme expression. *Biochim. Biophys. Acta.* 1083:121–134.

39. Ignarro, L., and K. Wood. 1987. Activation of purified soluble guanylate cyclase by arachidonic acid requires absence of enzyme-bound heme. *Biochim. Biophys. Acta.* 928:160–170.

40. Amano, Y., S. Lee, and A. Allison. 1991. Inhibition by glucocorticoids of the formation of interleukin-1a, interleukin-1b, and interleukin-6: mediation by decreased mRNA stability. *Mol. Pharmacol.* 43:176–182.

41. Huang, K.S., B.P. Wallner, R.J. Mattaliano, R. Tizard, C. Burne, A. Frey, C. Hession, P. McGray, L.K. Sinclair, E.P. Chow et al. 1986. Two human 35 kd inhibitors of phospholipase A2 are related to substrates of pp60v-src and of the epidermal growth factor receptor/kinase. *Cell.* 46:191–199.

42. Hussain, S., R. Graham, F. Rutledge, and C. Roussos. 1986. Respiratory muscle energetics during endotoxic shock in dogs. *J. Appl. Physiol.* 60:486–493.

43. Hirano, S. 1996. Migratory responses of PMN after intraperitoneal and intratracheal administration of lipopolysaccharide. *Am. J. Physiol.* 270:836–845.

44. Tracey, W., J. Tse, and G. Crater. 1995. Lipopolysaccharide-induced changes in plasma nitrite and nitrated concentration in rats and mice: pharmacological evaluation of nitric oxide synthase inhibitors. *J. Pharmacol. Exp. Ther.* 272:1011–1015.

45. Buttery, L., T. Evans, D. Springall, A. Carpenter, J. Cohen, and J. Polak. 1994. Immunochemical localization of inducible nitric oxide synthase in endotoxin-treated rats. *Lab. Invest.* 71:755–764.

46. Cunha, F., J. Assreuy, D. Moss, D. Ress, M. Leals, S. Moncada, M. Carrier, C. O'Donnel, and F. Liew. 1994. Differential induction of nitric oxide synthase in various organs of the mouse during endotoxemia: role of TNF-alpha and IL-1-β. *Immunology.* 81:211–215.

47. Piotrovskij, V., Z. Kallay, T. Trnovec, G. Krumpl, and K. Krejcy. 1994. Dose-ranging study of NG-nitro-L-arginine pharmacokinetics in rats after bolus intravenous administration. *Xenobiotica.* 24:663–669.

48. Tabrizi-Fard, M., and H.-L. Fung. 1994. Pharmacokinetics, plasma protein binding and urinary excretion of Nω-nitro-L-arginine in rats. *Br. J. Pharmacol.* 111:394–396.

49. Olken, N., and M. Marletta. 1992. NG-Allyl- and NG-Cyclopropyl-L-arginine: two novel inhibitors of macrophage nitric oxide synthase. *J. Med. Chem.* 35:1137–1144.

50. Reif, D., and S. McCreedy. 1995. *N*-nitro-L-arginine and *N*-monomethyl-L-arginine exhibit a different pattern of inactivation toward the three nitric oxide synthases. *Arch. Biochem. Biophys.* 320:170–176.

51. Rochester, D.F. 1985. The diaphragm: contractile properties and fatigue. *J. Clin. Invest.* 75:1397–1402.

52. Boczkowski, J., and M. Aubier. 1995. The respiratory muscle in sepsis. *In* The Thorax Part B. C. Roussos, editor. Marcell Dekker Inc., New York. 1483–1514.

53. Lancaster, J. 1994. Simulation of the diffusion and reaction of endogenously produced nitric oxide. *Proc. Natl. Acad. Sci. USA.* 91:8137–8141.

54. Vanderkooi, J., W. Wright, and M. Erecinska. 1994. Nitric oxide diffusion coefficients in solutions, proteins and membranes determined by phosphorescence. *Biochim. Biophys. Acta.* 1207:249–254.

55. Ungureanu-Longrois, D., J.-L. Balligand, I. Okada, W. Simmons, L. Kobzik, C. Lowestein, S. Kunkel, T. Michel, R. Kelly, and T. Smith. 1995. Contractile responsiveness of ventricular myocytes to isoproterenol is regulated by induction of nitric oxide synthase activity in cardiac microvascular endothelial cells in heterotypic primary culture. *Circ. Res.* 77:486–493.

56. Bolanos, J., S. Peuchen, S. Heales, J. Land, and J. Clark. 1994. Nitric oxide-mediated inhibition of the mitochondrial respiratory chain in cultured astrocytes. *J. Neurochem.* 63:910–916.

57. Cleeter, M., J. Cooper, V. Darley-Usmar, S. Moncada, and A. Schapira. 1994. Reversible inhibition of cytochrome C oxidase, the terminal enzyme of the mitochondrial respiratory chain, by nitric oxide. *FEBS Lett.* 345:50–54.